Communication

Mineral Identification based on Deep Learning that Combines Image and Mohs Hardness

Xiang Zeng [1], Yancong Xiao [1], Xiaohui Ji [1,*] and Gongwen Wang [2]

[1] School of Information Engineering, China University of Geosciences, Beijing 100083, China;
[2] School of Earth Sciences and Resources, China University of Geosciences, Beijing 100083, China;
* Correspondence: xhji@cugb.edu.cn;

Abstract: Mineral identification is an important part of geological analysis. Traditional identification methods rely on either the experiences of the appraisers or the various measuring instruments and the methods are either easily influenced by the experiences or need too much work. To solve the above problems, there have been studies using image recognition and intelligent algorithms to identify minerals. But the current studies can not identify many minerals, and the accuracy is low. To increase the number of identified mineral categories and the accuracy, we proposed the method that uses both the mineral images and the Mohs hardness in the deep neural networks to identify the minerals. The experimental results showed that the method can reach 94.0% Top-1 accuracy and 99.9% Top-5 accuracy for 28 common minerals. The model that combines image and Mohs hardness together can identify more minerals and increase the accuracy using less training data.

Keywords: mineral identification; deep learning; convolutional neural network; image; Mohs hardness

1. Introduction

Mineral identification is an important part of geological analysis. Traditional mineral identification is mainly based on visual observation or physical experiments [1]. Visual observation depends on the experience of the appraiser, and physical experiments requires special instruments. Both of the methods need a lot of labor work. Deep learning has been used in geosciences to reduce the labor work like the studies of [2-5]. In mineral identification, intelligent algorithm also has been used [1].

The current research on the intelligent identification of rocks and minerals can be divided into two categories, traditional identification and neural network identification. The traditional identification methods include laser-induced breakdown spectroscopy [6], color tracking [7], cascade approach [8], optimal spherical neighborhoods [9,10] and image processing and analysis [11], etc. The neural network methods identify minerals by using the digital features or the image features. The work of [12,13] and so on used the digital features. Spectral images, microscopic images, and photo images all can be used to identify the minerals. The work of [14] used spectral images to identify the minerals and achieved an accuracy of 83% for 6 types of minerals. By using the microscope image, the work of [15] identified the basaltic rock with an accuracy of 92.2%, [16] achieved an accuracy of 98.5% for 3 types of rocks, [17] identified 4 types of rocks and minerals with an accuracy of 90.9%, [18] achieved an accuracy of 93.86% for 5 types of minerals. The researches using the photo images include [19] achieving 91% accuracy for 6 types of rocks, [20] identifying 6 types of rocks with an accuracy of 96% and [21] achieving 74.2% accuracy for 12 types of rocks.

The above researches have been able to identify rocks and minerals automatically, but either the number of minerals identified or the accuracy achieved needs to be improved further.

One difficulty in identifying minerals using photo image is that the minerals in the same category may have variable colors and shapes, but the minerals in the different categories may have similar colors, shapes, and textures. Not only in mineral identification, but also in other applications, it is difficult to achieve a high accuracy by using only a single feature. Researches that use multiple features to improve the accuracy have appeared. For example, [22] combined word-level and char-level features to extract more information and improve accuracy in natural language processing, [23] combined the original image with the grayscale image and the text features in the breast cancer detection.

Hardness is an important property of minerals, and the Mohs hardness is used as a standard in the identification of jewelry and minerals [24,25]. The Mohs hardness can be easily measured by a portable tester, different types of minerals may have very different Mohs hardness. For example for hematite and sphalerite, which have very similar photo image, are in different Mohs hardness range. Hematite is in the range of 5.0-6.5, and sphalerite is in the range of 3.5-4.0. So the hardness of hematite and sphalerite can be used as the key information to distinguish them.

In this paper, hardness was combined with photo images in deep neural networks to identify minerals. The deep neural network can be trained at once which does not increase the training difficulty. Experiments on 28 types of common minerals showed that the proposed method can achieve 94.0% Top-1 accuracy and 99.9% Top-5 accuracy.

2. Data

The mineral photo images used in the paper are from Mindat (A mineral database) [26] and obtained by using a web spider. Mindat is a mineral database with all categories and great number of samples. All the mineral photo images on the database are from all over the world and have been identified. This paper uses all the 28 categories of the minerals.

All the obtained mineral images are cleaned manually, including removing bad data and cropping the images, so that the mineral in the main part of the image is consistent with its label. Bad data are those images that have no minerals, got from the microscope, or do not match the label. Examples of cropped images is shown in Figure 1. The 35,631 images got after cleaning were evenly mixed and separated as the training set, validation set and test set in the ratio of 8:1:1 in our neuron network identification.

The hardness of the real mineral can be obtained by the portable tester [24,25]. Mohs hardness is a value between 1 and 10 and the larger the value is, the higher the hardness of the mineral is [24,25]. In order to obtain the hardness of the mineral image, a random value within the range shown in Table 1 is set. The average of the random hardness of each category is the midpoint of the range in Table 1, and the random value follows a normal distribution with a standard deviation of 0.2.

3. Method

The method proposed in this paper is shown in Figure 2, which has three parts: image feature extraction (Figure 2(1)), hardness dimension increase (Figure 2(2)), and image and hardness features combination (Figure 2(3)).

Figure 1. Examples of cropped images (a~d Aquamarine, e~h Cinnabar, i~l Sphalerite, and m~p Pyrite)

The image feature extraction in Figure 2(1) uses deep convolutional neural network EfficientNet-b4 [27]. EfficientNet-b4 extracts image features automatically and extends the convolutional neural network in three dimensions of width, depth and image resolution, so it has fewer parameters and a higher Top-1 accuracy [27]. Because the sizes of the mineral images to be identified are different, they are uniformly scaled to the standard input size of 380×380 of EfficientNet-b4.

Hardness dimension increase in Figure 2(2) is to transform the Mohs hardness from a value into a vector by using two fully connected layers of dimension 28 and 1024. Then the vector is concatenated with the image feature vector output by the EfficientNet-b4. ReLu activation function [28] is also added after the fully connected layer to introduce nonlinearity, so that more information can be extracted from the hardness.

Combination of image and hardness features in Figure 2(3) uses a fully connected layer to get the final result. Fully connected layers, instead of other classification methods like support vector machines or decision trees, is used is to enable the training to be completed at once. Otherwise, the training of image feature extraction, hardness feature extraction and the final prediction classification have to be done separately for three times. When training the neural network in Figure 2, data augmentation and transfer learning are adopted. Data augmentation is to enhance the generalization ability of the model to identify the minerals untrained more accurately, which is implemented by flipping, cropping, zooming, and changing the contrast

and brightness of the trained images randomly. Transfer learning uses the pre-trained weights of ImageNet [29] as the initial weights, which greatly speeds up the convergence of the model compared with the random initialization weights. The normalized mean and standard deviation used in training are the same as that in ImageNet and the optimizer used is Adam. The learning rate decays from 10^{-3} to 10^{-4} exponentially. The loss function used is Focal Loss (FL) [30] to solve the problem of category imbalance caused by the differences of the number of images of different types of minerals. The number of training epochs is set as 50, and the gradient descent algorithm is used to update the parameters of the model. The accuracy and the cross-entropy loss curves on the training and the validation set are shown in Figure 3. From Figure 3 we can see that curves using both image and hardness converge faster than the curves using image only.

Table 1. Name of the mineral category, its range of Mohs hardness and the number of samples

#	Mineral category	Mohs hardness range	Number of samples
1	Agate	6.5-7.0	2054
2	Albite	6.0-6.5	1158
3	Almandine	7.0-7.5	1511
4	Aquamarine	7.5-8.0	1351
5	Azurite	3.5-4.0	1902
6	Chalcopyrite	3.5-4.0	1202
7	Cinnabar	2.0-2.5	896
8	Copper	3.0-3.0	1224
9	Corundum	2.0-2.5	1522
10	Demantoid	6.5-7.0	694
11	Epidote	6.0-7.0	1900
12	Fluorite	4.0-4.0	1735
13	Galena	3.5-4.0	1461
14	Gold	2.5-3.0	1253
15	Halite	2.0-2.5	570
16	Hematite	5.0-6.5	1028
17	Malachite	3.5-4.0	1482
18	Marcasite	6.0-6.5	902
19	Opal	5.5-6.5	1221
20	Orpiment	1.5-2.0	608
21	Pyrite	6.0-6.5	1239
22	Pyroxene Group	5.0-7.0	1253
23	Quartz	7.0-7.0	1328
24	Sphalerite	3.5-4.0	1322
25	Stibnite	2.0-2.0	1272
26	Sulphur	1.5-2.5	1152
27	Topaz	8.0-8.0	1137
28	Wulfenite	2.5-3.0	1254

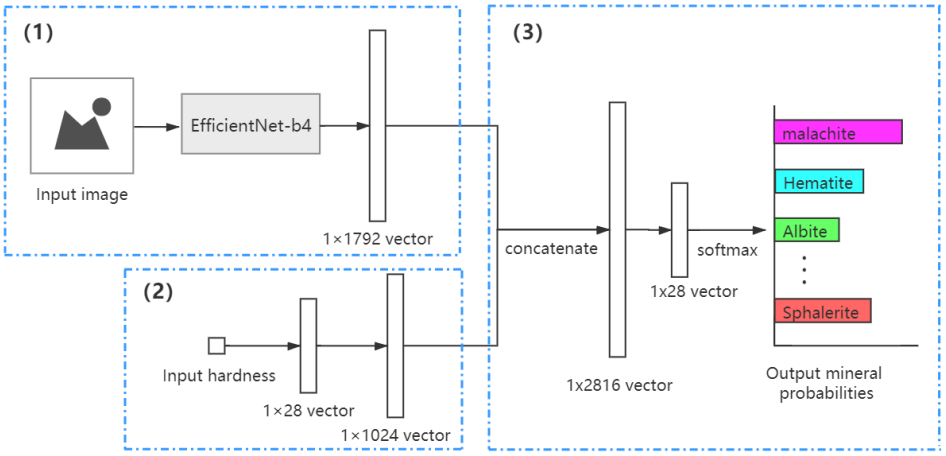

Figure 2. Mineral identification using image and Mohs hardness

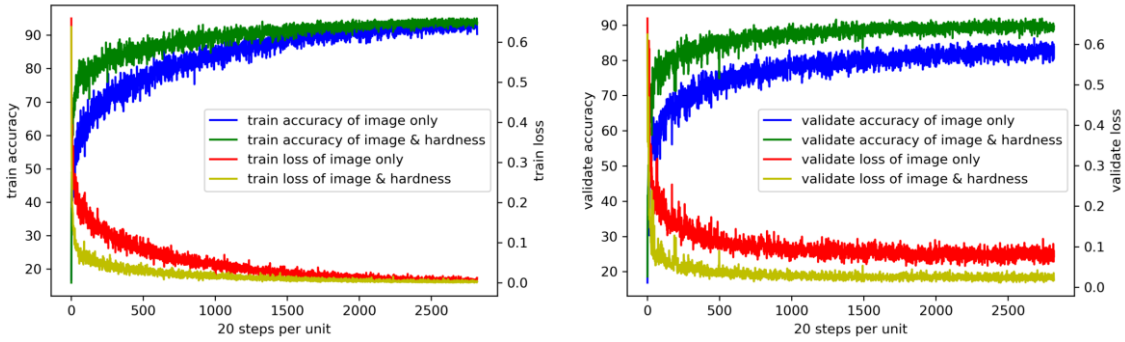

Figure 3. Accuracy and cross-entropy loss curves on the training set (left) and validation set (right)

4. Results and Discussion

This section gives the results of our work and its comparison with other methods.

4.1. Our experimental results

Accuracy and Confusion Matrix [31] were used to test our method. Experiments using image only (EfficientNet-b4 neural network is used), using hardness only (a fully connected network is used) and using both image and hardness (the ensembled network shown in Figure 2 is used) were carried out. The experimental results of the accuracy are shown in Table 2, in which Top-1 accuracy means that the model result with the highest probability is exactly the mineral to be identified, and Top-5 accuracy means that one of the 5 most likely results given by the model must match the identified mineral. Table 2 indicates that the combination of the image and the hardness can greatly improve the accuracy of Top-1. Comparison of accuracy of specific mineral types is shown in Figure 4. We can see that after adding the hardness, the accuracy of almost all mineral types are improved, especially for the category 2, 6 12, 16, 20, 22, 23, 27, and 28, which were improved by more than 15%. The main reason is that the shapes, textures and colors of many minerals are similar to quartz, or are often associated with quartz [32]. So quartz often appears in the image, which makes it difficult for the model to identify the minerals correctly only based on images. The only category that the accuracy was reduced after adding the hardness is No.17, malachite, whose accuracy is reduced by 2.5%. This is because there are 4 other categories of minerals, azurite, chalcopyrite, galena and sphalerite, overlap their hardness range with malachite.

Table 2. Comparison of the accuracy of our three methods

Method	Top-1 accuracy(%)	Top-5 accuracy(%)
hardness only	30.7	93.5
image only	84.1	98.3
image & hardness	***94.0***	***99.9***

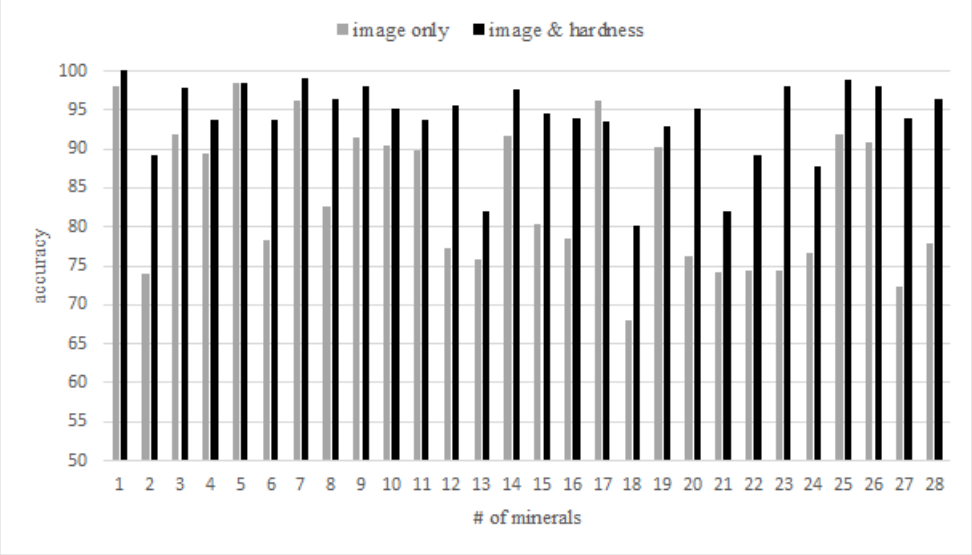

Figure 4. Comparison of accuracy of specific mineral types

The confusion matrix using image only and the combination of image and hardness are shown in Figure 5. From Figure 5 we can see that adding hardness is beneficial to improve the accuracy of mineral identification. Because if the amplitude of the grids on the confusion matrix diagonal is larger (in darker color generally), the result has a higher accuracy. The smaller the amplitude of the grids outside the diagonal (in lighter colors generally), the lower the probability of the wrong identification and the better the model performs. Compared with the left in Figure 5, the diagonal color in the right is darkened, and the colors of the other grids are general lighter, which shows that the accuracy of the model was improved significantly by adding hardness.

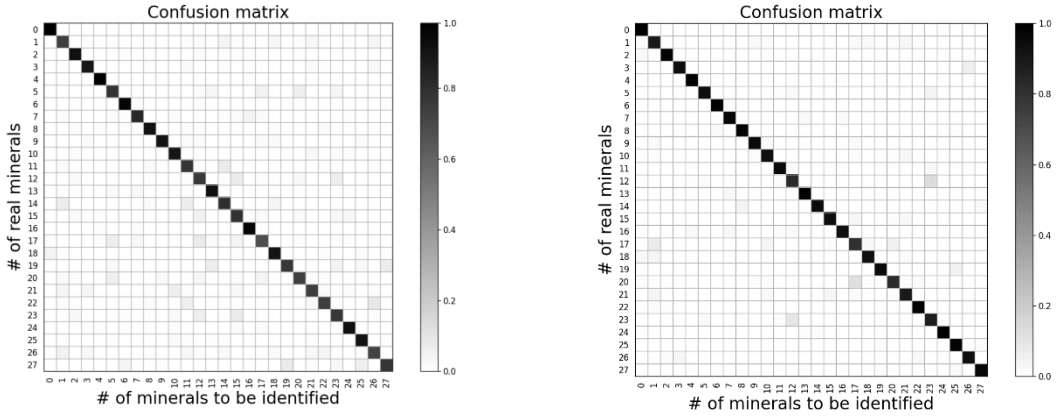

Figure 5. Confusion matrix of using image only (left) and using image & hardness (right)

4.2. Comparison with other methods

Table 3 shows the comparison of the number of identified categories, the accuracy, the amount of data used in training and testing of the related researches. Compared with the method that uses spectral images like the work of [14]Ishikawa and Gulick (2013), which can only identify 6 categories of minerals, our method can identify 28 categories of minerals with higher accuracy. On the other hand, our method does not require the special instruments to obtain the spectral data, the Mohs hardness we need can be obtained by a portable tester easily. Compared with the studies of [16-18]Cheng et al. (2017), Zhang et al. (2019), and Baykan and Yilmaz (2011) whose work use microscopic image, our work do not need any microscope, and the number of categories identified increased from 3, 4 and 5 to 28. The accuracy is also higher for most minerals. Compared with the studies of [19]Solar et al. (2008), [20] and [21]Liu et al. (2020) whose work use photo images only, our work increases the number of identified categories to 28 , and the accuracy improved 3.0% and 19.8% for the work of [19] and [21]Solar et al. (2008).

Table 3. Comparison of the work in Mineral Identification Using Images

Image type	Researches	Performance		Amount of Data	
		Number of identified categories	Accuracy (%)	Training	Testing
spectral	[14]	6	83.0	190	167
microscope	[16]	3	98.5	3600	1200
	[17]	4	90.9	480	/
	[18]	5	93.9	400	
photo	[19]	6	91.0	160	240
	[20]	8	96.0	70329	7814
	[21]	12	74.2	4178	440
photo & hardness	Our method	***28***	94.0	32067	3563

In Table 3, [20][21] and our work use deep neuron network, and the larger the training data used the higher accuracy was achieved. Averagely, [20] used 70329/8=8791 training data per category, [21] used 4178/12=348 training data per category and our work used 32067/28=1145 training data per category. So 13% training data of [20] was used to identify one category of the minerals with almost the same accuracy. On one hand, this is because the hardness is used in our work. On the other hand, the neuron network we use in processing the photos is EfficientNet-b4 that needs less data and has higher accuracy than VGG-16 that was used in [20]. By using more training data our work can get higher accuracy.

5. Conclusions

In this paper, a mineral identification method based on deep learning that combines image and hardness together is proposed. Compared with the traditional visual or microscope observation, the proposed method reduces the reliance on experienced experts and the workload is low. Compared with the method that uses mineral images only, our method that combines the Mohs hardness identifies more minerals and improves the accuracy greatly with much less training data. By using a camera to take a photo and using a portable tester to get the mohs hardness of the mineral, we can identify it easily, timely and accurately, which provides a

reliable method for mineral identification, especially in the field. In the future, more features such as density, gloss, cleavage, etc. can be introduced to improve the accuracy further.

Author Contributions: Conceptualization, Xiang Zeng and Xiaohui Ji; methodology, Xiang Zeng and Yancong Xiao; software, Xiang Zeng and Yancong Xiao; validation, Xiaohui Ji and Gongwen Wang; writing—original draft preparation, Xiang Zeng; writing—review and editing, Xiaohui Ji. All authors have read and agreed to the published version of the manuscript.

Funding: This research was funded by Project of Transformation of Scientific and Technological Achievements of China University of Geosciences, Beijing.

Conflicts of Interest: The authors declare no conflict of interest. The funders had no role in the design of the study; in the collection, analyses, or interpretation of data; in the writing of the manuscript, or in the decision to publish the results.

References

1. Baklanova, O. E.; Baklanov, M. A. Methods and algorithms of image recognition for mineral rocks in the mining industry. Proceedings of International Conference on Swarm Intelligence, 2016, 253-262.
2. Porwal, A.; Carranza, E.; Hale, M. Artificial neural networks for mineral-potential mapping: a case study from Aravalli Province, Western India. *Natural Resources Research* **2003**, 12, 155-171.
3. Karimpouli, S.; Tahmasebi, P.; Saenger, E. H. Coal cleat/fracture segmentation using convolutional neural networks. *Natural Resources Research* **2019**, 1-11.
4. Juliani, C.; Ellefmo, S.L. Prospectivity Mapping of Mineral Deposits in Northern Norway Using Radial Basis Function Neural Networks. *Minerals* **2019**, 9, 131.
5. Sun, T.; Li, H.; Wu, K.; Chen, F.; Hu, Z. Data-driven predictive modelling of mineral prospectivity using machine learning and deep learning methods: a case study from southern jiangxi province, china. *Minerals* **2020**, 10, 102.
6. El Haddad, J.; de Lima Filho, E. S.; Vanier, F.; Harhira, A.; Padioleau, C.; Sabsabi, M. et al. Multiphase mineral identification and quantification by laser-induced breakdown spectroscopy. *Minerals Engineering* **2019**, 134, 281-290.
7. Aligholi, S.; Lashkaripour, G. R.; Khajavi, R.; Razmara, M. Automatic mineral identification using color tracking. *Pattern Recognition* **2017**, 65, 164-174.
8. Izadi, H.; Sadri, J.; Bayati, M. An intelligent system for mineral identification in thin sections based on a cascade approach. *Computers & geosciences* **2017**, 99, 37-49.
9. Młynarczuk, M.; Górszczyk, A.; Ślipek, B. The application of pattern recognition in the automatic classification of microscopic rock images. *Computers & geosciences* **2013**, 60, 126-133.
10. Ślipek, B.; Młynarczuk, M. Application of pattern recognition methods to automatic identification of microscopic images of rocks registered under different polarization and lighting conditions. *Geology, Geophysics and Environment* **2013**, 39, 373.
11. Aligholi, S.; Khajavi, R.; Razmara, M. Automated mineral identification algorithm using optical properties of crystals. *Computers & geosciences* **2015**, 85, 175-183.
12. Harris, D.; Pan, G. Mineral favorability mapping: a comparison of artificial neural networks, logistic regression, and discriminant analysis. *Natural Resources Research* **1999**, 8, 93-109.
13. Thompson, S.; Fueten, F.; Bockus, D. Mineral identification using artificial neural networks and the rotating polarizer stage. *Computers & geosciences* **2001**, 27, 1081-1089.
14. Ishikawa, S. T.; Gulick, V. C. An automated mineral classifier using Raman spectra. *Computers & geosciences* **2013**, 54, 259-268.
15. Singh, N.; Singh, T.; Tiwary, A.; Sarkar, K. M. Textural identification of basaltic rock mass using image processing and neural network. *Computational Geosciences* **2010**, 14, 301-310.
16. Cheng, G.; Guo, W. Rock images classification by using deep convolution neural network. In Journal of Physics: Conference Series, 2017.
17. Zhang, Y.; Li, M.; Han, S.; Ren, Q.; Shi, J. Intelligent Identification for Rock-Mineral Microscopic Images Using Ensemble Machine Learning Algorithms. *Sensors* **2019**, 18, 3914.
18. Baykan, N. A.; Yılmaz, N. A mineral classification system with multiple artificial neural network using k-fold cross validation. *Mathematical and Computational Applications* **2011**, 16, 22-30.

19. Solar, M.; Perez, P.; Watkins, F. Neural Recognition of Minerals. Proceedings of Artificial Intelligence in Theory and Practice, 2008; 433-437.
20. Liu, X.; Wang, H.; Jing, H.; Shao, A.; Wang, L. Research on Intelligent Identification of Rock Types Based on Faster R-CNN Method. *IEEE Access* **2020**, 8, 21804-21812.
21. Liu, C.; Li, M.; Zhang, Y.; Han, S.; Zhu, Y. An Enhanced Rock Mineral Recognition Method Integrating a Deep Learning Model and Clustering Algorithm. *Minerals* **2019**, 9, 516.
22. Wang, J.; Wang, Z.; Zhang, D.; Yan, J. Combining Knowledge with Deep Convolutional Neural Networks for Short Text Classification. Proceedings of the International Joint Conference on Artificial Intelligence, 2017; 2915-2921.
23. Hai, J.; Tan, H.; Chen, J.; Wu, M.; Qiao, K.; Xu, J., et al. Multi-level features combined end-to-end learning for automated pathological grading of breast cancer on digital mammograms. *Computerized Medical Imaging and Graphics* **2019**, 71, 58-66.
24. Tabor, D. Mohs's hardness scale-a physical interpretation. Proceedings of the Physical Society, 1954, Section B, 67, 249.
25. Administration, U. S. F. H. Rock and mineral identification for engineers: U.S. Dept. of Transportation, Federal Highway Administration, 1991.
26. A mineral database. Available online: https://www.mindat.org/ (accessed on 4th August, 2020).
27. Tan, M.; Le, Q. V. Efficientnet: Rethinking model scaling for convolutional neural networks. Proceedings of the 36th international conference on machine learning (ICML-19), 2019.
28. Nair, V.; Hinton, G. E. Rectified linear units improve restricted boltzmann machines. Proceedings of the 27th international conference on machine learning (ICML-10), 2010; 807-814.
29. Deng, J.; Dong, W.; Socher; R.; Li, L.-J.; Li, K.; Li F.-F. Imagenet: A large-scale hierarchical image database. Proceedings of 2009 IEEE conference on computer vision and pattern recognition, 2009; 248-255.
30. Lin, T.-Y.; Goyal, P.; Girshick, R.; He, K.; Dollár, P. Focal loss for dense object detection. Proceedings of the IEEE international conference on computer vision, 2017; 2980-2988.
31. Tharwat, A. Classification assessment methods. *Applied Computing and Informatics* 2018.
32. Howie R. A. *The Ore Minerals and Their Intergrowths*, 2nd ed., Pergamon press, 1980.